ELSEVIER

Polymer 41 (2000) 5257–5267

polymer

Lattice fluid theory in the analysis of interaction parameters and phase behaviour of blends involving copolymers of cyclohexyl methacrylate, methyl methacrylate and various styrene derivatives

A. Múgica, P.M. Remiro, M. Cortázar*

Departamento de Ciencia y Tecnología de Polímeros, Facultad de Ciencias Químicas de San Sebastián, P.O. Box 1072, E-20018, San Sebastián, Spain

Received 15 June 1999; received in revised form 16 September 1999; accepted 27 September 1999

Abstract

The phase behaviour and interaction parameters of binary blends of copolymers involving cyclohexyl methacrylate (CHMA), methyl methacrylate (MMA) and various styrene derivatives (styrene (S), α-methylstyrene (AMS) and *p*-methylstyrene (PMS)) are examined using the lattice fluid theory of Sanchez and Lacombe. 'Bare' interaction parameters (ΔP_{ij}^{*}) for various monomer unit pairs were deduced where possible from lower critical solution temperature (LCST) type phase boundaries and from a binary interaction model. The calculations reveal that values of the interaction parameters are less favourable to miscibility when PMS is employed instead of S in blends with CHMA and MMA. These data are in good agreement with the experimental results and the interaction parameters obtained are translatable from one system to another. The results are discussed in terms of interactions between monomer unit pairs, equation-of-state effects and thermodynamical properties. © 2000 Elsevier Science Ltd. All rights reserved.

Keywords: Blends; Lattice fluid theory; Phase diagrams

1. Introduction

In those polymer blends where interactions are weak the miscibility behaviour can be significantly influenced by small changes in size and shape of the constituent monomer. An illustrative example [1–3] is the miscibility behaviour of the polystyrene–polymethacrylate blends. Polystyrene is immiscible with some polyalkylmethacrylates (methyl, *n*-buthyl, *t*-buthyl) whereas it is miscible with others (ethyl, *n*-propyl, cyclohexyl). This effect is a consequence of changes in the intermolecular packing of blend components that can affect the degree of enthalpic interaction as well as the so-called noncombinatorial entropy of the system [4,5]. Classical Flory–Huggins lattice theory [6] does not take into account the noncombinatorial entropy arising from the free volume effects and cannot explain the lower critical solution temperature (LCST) behaviour exhibited by many polymer blends. This problem can be overcome by assigning temperature dependence to the interaction energy [7,8]. With this modification, the Flory–Huggins equation can be useful because it requires few experimental parameters. However, the interaction energies so calculated are only overall quantities and therefore it is difficult to understand their molecular meaning.

The equation of state theories account for the effects of compressibility, or free volume and therefore represent more properly the LCST behaviour of polymer blends than does the empirically modified Flory–Huggins theory [9–16]. From accurate LCST data, mixture parameters that characterize the polymer–polymer interaction energies can be obtained. Despite the fact that these interaction energies are required for prediction of the thermodynamical properties of new polymer mixtures, there are too few data in the literature to achieve a detailed molecular understanding of them. By manipulating appropriately the copolymer composition of mixtures, the interaction level needed to obtain phase separation temperatures, LCST, across a wide range of copolymer compositions can be achieved. From these data intersegmental interaction parameters of interest can be calculated [14–16]. A practical and definitive way to probe the usefulness and the reliability of the calculated interaction parameters can be to examine the predictions about miscibility–immiscibility boundaries of new polymer blends in which the calculated parameters are involved.

In this paper, we examine the effect of small changes in the monomer repeat unit on the phase behaviour of binary blends involving the polymethacrylate copolymer and

---

* Corresponding author. Tel.: +34-9-4301-8189; fax: +34-9-4321-2236.
E-mail address: popcodim@sq.ehu.es (M. Cortázar).

PII: S0032-3861(99)00742-9

polystyrene derivatives, polystyrene (PS), poly(α(methylstyrene) (PAMS), and poly(*p*-methylstyrene) (PPMS). The Sanchez-Lacombe lattice fluid theory combined with a binary interaction model [17–19] has been employed to evaluate the characteristic interaction energy density of the moiety pairs involved, ΔP^*_{ij}, defined as a 'bare' interaction energy density without free volume effects. Furthermore, theoretical miscibility windows for binary blends of copolymers involving MMA, CHMA and styrene derivatives have been checked against experimental results as a way to probe whether minor differences in the styrene repeat unit can be well-described by the lattice fluid theory. Finally, the Flory–Huggins binary interaction energy B_{ij} has been examined in terms of the Sanchez–Lacombe compressible model. The B_{ij} temperature dependence has been determined for various monomer pairs, as has the temperature dependence of its enthalpic and entropic components.

2. Theoretical background

In contrast to Flory–Huggins theory, the Sanchez–Lacombe lattice fluid theory includes vacant lattice sites to take into account the different compressibilities of the components in the mixture [12,13]. The Sanchez–Lacombe equation of state is given by

$$\tilde{\rho}^2 + \tilde{P} + \tilde{T}\left[\ln(1-\tilde{\rho}) + \left(1 - \frac{1}{r}\right)\tilde{\rho}\right] = 0 \tag{1}$$

where the reduced properties are defined as $\tilde{P} = P/P^*$, $\tilde{T} = T/T^*$ and $\tilde{\rho} = v^*/v$ and r is a chain length parameter proportional to molecular weight, M, defined as

$$r = \frac{MP^*}{\mathrm{k}T^*\rho^*} = \frac{M}{\rho^* v^*} \tag{2}$$

where k is the Boltzman constant and P^*, T^*, ρ^* (or v^*) are the characteristic parameters of a polymer component which can be obtained by fitting PVT data to Eq. (1). For the extension of the lattice fluid theory to mixtures and copolymers some appropriate combing rules which are given by Sanchez and Lacombe [13] are required. In this theoretical model, each pure component has its own unique mer volume v_i^*, whereas in the mixture all mers are required to have the same average close-packed volume v^*. Thus, if an i molecule occupies r_i^0 sites and has a volume of $r_i^0 v_i^*$ in the pure state, then in the mixture it will occupy r_i sites such that $r_i^0 v_i^* = r_i v^*$. The rest of the mixing rules are described as follows:

$$\frac{1}{v^*} = \sum_i \frac{\phi_i}{v_i^*};\quad \frac{1}{\rho^*} = \sum_i \frac{w_i}{\rho_i^*};\quad \frac{1}{r} = \sum_i \frac{\phi_i}{r_i}; \tag{3}$$

where w_i is the weight fraction of component i and ϕ_i is the hard-core volume fraction which for a binary system (1, 2) could be calculated using

$$\phi_i = \frac{w_1/\rho_1^*}{w_1/\rho_1^* + w_2/\rho_2^*} \tag{4}$$

with $\phi_2 = 1 - \phi_1$. Finally, the characteristic pressure of a two-component system is

$$P^* = \phi_1 P_1^* + \phi_2 P_2^* - \phi_1\phi_2\Delta P^* \tag{5}$$

with ΔP^* being the net bare interaction energy of the mixture. To describe miscibility of random copolymer blends, lattice fluid theory has been combined with the binary interaction model [17–19]. According to this model, for a binary blend of a copolymer composed of units A and B and a homopolymer composed of unit C, ΔP^* can be written as

$$\Delta P^* = \phi'_{\mathrm{A}}\Delta P^*_{\mathrm{AC}} + \phi'_{\mathrm{B}}\Delta P^*_{\mathrm{BC}} - \phi'_{\mathrm{A}}\phi'_{\mathrm{B}}\Delta P^*_{\mathrm{AB}} \tag{6}$$

where ϕ'_{A} and ϕ'_{B} are the close-packed volume fractions of units A and B in the copolymer and can be calculated using appropriately Eq. (4). ΔP^*_{ij} is the binary pair interaction energy between i and j units. The mixture will be stable if the second derivative of Gibbs free energy with respect to composition is positive over the entire composition range, i.e.

$$\frac{\mathrm{d}^2G}{\mathrm{d}\phi_1^2} = \frac{1}{2}\left(\frac{1}{r_1\phi_1} + \frac{1}{r_2\phi_2}\right) - \tilde{\rho}\left(\frac{\Delta P^* v^*}{\mathrm{k}T} + \frac{1}{2}\psi^2\tilde{T}P^*\beta\right) > 0 \tag{7}$$

where

$$\Psi = \frac{\left\{\tilde{\rho}\left[\nu\left(\frac{1}{\tilde{T}_1} - \frac{1}{\tilde{T}_2}\right) + \frac{\left(\phi_1^2 - \nu\phi_2^2\right)\Delta P^* v_1}{\mathrm{k}T}\right] - \nu\left(\frac{1}{r_1^0} - \frac{1}{r_2^0}\right) + \frac{\tilde{P}\tilde{v}}{\tilde{T}}(\nu - 1)(\phi_1 + \nu\phi_2)\right\}}{(\phi_1 + \nu\phi_2)^2} \tag{8}$$

ν is the pure polymer hard-core volume relation so $\nu = v_1^*/v_2^*$, r_i is the chain length of the i polymer in the mixture and r_i^o is the chain length of i polymer in the pure state. β is the mixture isothermal compressibility

$$\tilde{T}P^*\beta = \frac{\tilde{v}}{\frac{1}{\tilde{v}-1} + \frac{1}{r} - \frac{2}{\tilde{v}\tilde{T}}} \tag{9}$$

A temperature-dependent interaction energy $B(T)$ can be incorporated in the Flory–Huggins treatment through the empirical expresion $B(T) = B^{\mathrm{h}} - TB^{\mathrm{s}}$ that includes besides an enthalpic contribution, other noncombinatorial entropic ones [7]. Both contributions can be written in terms of the Sanchez-Lacombe theory as shown by Kim and Paul [15,16]. The enthalpic contribution is given by

$$B^{\mathrm{h}} = \tilde{\rho}\Delta P^{*} + \left[\frac{P_1^{*}}{\phi_2}(\tilde{\rho}_1 - \tilde{\rho}) + \frac{P_2^{*}}{\phi_1}(\tilde{\rho}_2 - \tilde{\rho}) \right] + \frac{P^{*}}{\phi_1\phi_2}(\tilde{v} - \phi_1\tilde{v}_1 - \phi_2\tilde{v}_2) \qquad (10)$$

similarly, another relationship can be derived for the entropic part of B

$$-TB^{\mathrm{s}} = \frac{RT}{\phi_1\phi_2}\left\{ \frac{1}{v^{*}}\left[\frac{1-\tilde{\rho}}{\tilde{\rho}}\ln(1-\tilde{\rho}) + \frac{\ln\tilde{\rho}}{r} \right] - \frac{\phi_1}{v_1^{*}}\left[\frac{1-\tilde{\rho}_1}{\tilde{\rho}_1}\ln(1-\tilde{\rho}_1) + \frac{\ln\tilde{\rho}_1}{r_1^{0}} \right] - \frac{\phi_2}{v_2^{*}}\left[\frac{1-\tilde{\rho}_2}{\tilde{\rho}_2}\ln(1-\tilde{\rho}_2) + \frac{\ln\tilde{\rho}_2}{r_2^{0}} \right] \right\} \qquad (11)$$

In terms of Flory–Huggins theory the spinodal condition is given by

$$\mathrm{d}^2\Delta g/\mathrm{d}\phi_1^2 = RT/2\left(\frac{1}{\phi_1\tilde{v}_1} + \frac{1}{\phi_2\tilde{v}_2} \right) - B_{\mathrm{SC}} = 0 \qquad (12)$$

B_{sc} being the interaction parameter at the spinodal condition, that in terms of Sanchez–Lacombe theory can be written as:

$$B_{\mathrm{SC}} = \frac{\tilde{\rho}\Delta P^{*} + \left\{ P_2^{*} - P_1^{*} + (\phi_2 - \phi_1)\Delta P^{*} + \frac{RT}{\tilde{\rho}}\left[\frac{1}{r_1^{0}v_1^{*}} - \frac{1}{r_2^{0}v_2^{*}} \right] - RT\left[\frac{\ln(1-\tilde{\rho})}{\tilde{\rho}^2} + \frac{1}{\tilde{\rho}} \right]\left[\frac{1}{v_1^{*}} - \frac{1}{v_2^{*}} \right] \right\}^2}{\left\{ \frac{2RT}{v^{*}}\left[\frac{2\ln(1-\tilde{\rho})}{\tilde{\rho}^3} + \frac{1}{\tilde{\rho}^2(1-\tilde{\rho})} + \frac{1-1/r}{\tilde{\rho}^2} \right] \right\}} \qquad (13)$$

From the experimental spinodal curve, ΔP^{*} can be determined by means of Eq. (7) and for a copolymer blend the intersegmental parameters of the constituent monomer segments can be evaluated by means of Eq. (6). When ΔP^{*} is known, B^{s}, B^{h} and B_{sc} can be calculated from Eqs. (10)–(13).

3. Materials and procedures

Table 1 describes the polymers used in this study. Poly(α-methylstyrene) (PAMS) was supplied by Scientific Polymer Products, INC and PPMS by Aldrich. The polymerization and copolymerization of the monomers, (methyl methacrylate (MMA), cyclohexyl methacrylate (CHMA), styrene and *p*-methylstyrene) with each other were conducted in benzene solution at 70°C using azobisisobutyronitrile (AIBN) as the initiator. Random copolymers of different compositions were prepared by keeping the conversion less than 10% to minimize any composition drift. The samples were isolated by precipitation into cold methanol and afterwards purified by repeated precipitation from tetrahydrofuran (THF) solution into an excess of cold methanol. Then they were dried in a vacuum oven at 130°C for 2–3 days.

Polymer blends of 50/50 composition by weight were prepared by casting from THF at room temperature for one day; the polymer solution was poured onto covered glass plates with a small orifice from which the solvent could evaporate. Evaporation of the solvent took place slowly and produced smooth films. Before the samples were removed they were annealed in a vacuum oven at 130°C for up to 48 h. Copolymer compositions were determined by ^{1}H NMR, whereas molecular weight information was determined by gel permeation chromatography (GPC) calibrated with polystyrene standards and THF as the solvent. These values are shown in Table 1. Thermal stability of a number of polymers was determined using a DuPont 951 TG apparatus at 10°C min^{-1} under N_2 atmosphere, in order to establish their decomposition temperature, which was ~265°C.

Miscibility was judged by the T_{g} behaviour [20] determined using a Perkin–Elmer DSC-2 and DSC-7 at 20°C min^{-1} under N_2 atmosphere. The apparatus were calibrated using indium as a standard. Because of the close proximity of T_{g} values for some homopolymers and copolymers analysed, in many samples determining miscibility behaviour depended upon taking advantage of the phenomenon of enthalpy recovery [21] in physically aged samples. These samples were compared with physically mixed samples that received the same ageing treatment. The samples were annealed for one day at approximately 20°C below (~80°C) the temperature at which there was a change in specific heat in the scan without any previous thermal treatment. We obtained clear, well defined, enthalpy peaks in the next scan after the ageing treatment. Various thermograms describing the thermal treatment are shown in Fig. 1, where (a) and (b) correspond to systems judged as miscible and (c) and (d) systems judged as immiscible. The phase behaviour was also judged by cloud point measurements, which were measured by visual and thermo-optical analysis (TOA) using a hot stage (Mettler FP 82HT) equipped with a temperature controller (Mettler FP80) at a heating rate of 0.2°C min^{-1}. For the visual technique, the specimen was

Table 1
Copolymer compositons (determined from ^{1}H NMR) (wt%) and molecular weights of the polymers used in this study

Sample	$\bar{M}_n$[a] (kg/mol)	$\bar{M}_w$[a] (kg/mol)
Polystyrene	100	350
Poly(methyl methacrylate)	70	120
Poly(cyclohexyl methacrylate)	227	364
Poly(α-methylstyrene)	398	425
Poly(*p*-methylstyrene)	35	72
Poly(*p*-methylstyrene)	185	406
Poly(S$_{6}$-*co*-MMA$_{94}$)	246	418
Poly(S$_{27}$-*co*-MMA$_{73}$)	110	185
Poly(S$_{49}$-*co*-MMA$_{51}$)	96	145
Poly(S$_{62}$-*co*-MMA$_{38}$)	87	130
Poly(S$_{88}$-*co*-MMA$_{12}$)	115	195
Poly(S$_{90}$-*co*-MMA$_{10}$)	80	123
Poly(S$_{23}$-*co*-CHMA$_{77}$)	253	440
Poly(S$_{25}$-*co*-CHMA$_{75}$)	148	233
Poly(S$_{33}$-*co*-CHMA$_{67}$)	277	510
Poly(S$_{50}$-*co*-CHMA$_{50}$)	120	182
Poly(S$_{75}$-*co*-CHMA$_{25}$)	92	138
Poly(S$_{88}$-*co*-CHMA$_{12}$)	76	127
Poly(CHMA$_{91}$-*co*-MMA$_{9}$)	297	660
Poly(CHMA$_{81}$-*co*-MMA$_{19}$)	256	610
Poly(CHMA$_{78}$-*co*-MMA$_{22}$)	256	600
Poly(CHMA$_{73}$-*co*-MMA$_{27}$)	210	552
Poly(CHMA$_{64}$-*co*-MMA$_{36}$)	265	760
Poly(CHMA$_{53}$-*co*-MMA$_{47}$)	246	492
Poly(CHMA$_{50}$-*co*-MMA$_{50}$)	228	472
Poly(CHMA$_{48}$-*co*-MMA$_{52}$)	234	533
Poly(CHMA$_{41}$-*co*-MMA$_{59}$)	220	375
Poly(CHMA$_{36}$-*co*-MMA$_{64}$)	167	324
Poly(CHMA$_{30}$-*co*-MMA$_{70}$)	220	385
Poly(CHMA$_{28}$-*co*-MMA$_{72}$)	215	462
Poly(CHMA$_{24}$-*co*-MMA$_{76}$)	164	398
Poly(CHMA$_{18}$-*co*-MMA$_{82}$)	182	378
Poly(CHMA$_{12}$-*co*-MMA$_{88}$)	210	378
Poly(CHMA$_{8}$-*co*-MMA$_{92}$)	235	464
Poly(PMS$_{83}$-*co*-CHMA$_{17}$)	65	122
Poly(PMS$_{74}$-*co*-CHMA$_{26}$)	70	130
Poly(PMS$_{59}$-*co*-CHMA$_{41}$)	166	340
Poly(PMS$_{45}$-*co*-CHMA$_{55}$)	112	230
Poly(PMS$_{41}$-*co*-CHMA$_{59}$)	83	183
Poly(PMS$_{27}$-*co*-CHMA$_{73}$)	212	413
Poly(PMS$_{92}$-*co*-MMA$_{8}$)	54	105
Poly(PMS$_{77}$-*co*-MMA$_{23}$)	70	125
Poly(PMS$_{73}$-*co*-MMA$_{27}$)	70	130
Poly(PMS$_{54}$-*co*-MMA$_{46}$)	87	170
Poly(PMS$_{51}$-*co*-MMA$_{49}$)	90	165
Poly(PMS$_{40}$-*co*-MMA$_{60}$)	107	218
Poly(PMS$_{29}$-*co*-MMA$_{71}$)	96	190
Poly(PMS$_{26}$-*co*-MMA$_{74}$)	113	192

[a] From GPC calibrated by using polystyrene standards.

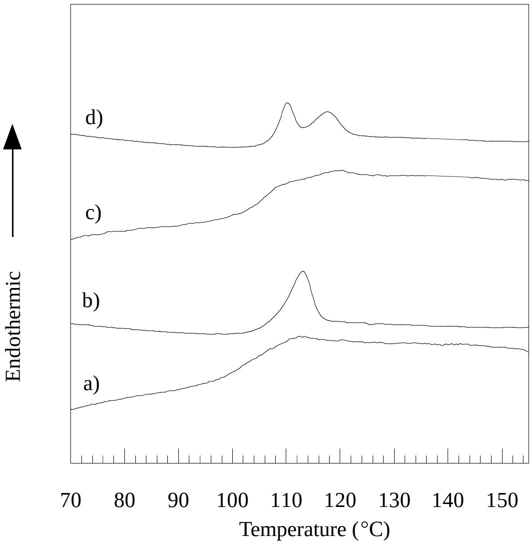

Fig. 1. DSC thermograms for P(CHMA$_{78}$-*co*-MMA$_{22}$)/P(S$_{62}$-*co*-MMA$_{38}$) (50/50) blend system: (a) without any thermal treatment; (b) after the ageing treatment. DSC thermograms for P(CHMA$_{78}$-*co*-MMA$_{22}$)/P(S$_{49}$-*co*-MMA$_{51}$) (50/50) blend system; (c) without any thermal treatment; and (d) after the ageing treatment.

covered with a glass slide, placed on a hot plate, and heated until it became cloudy. The temperature at which the blend first started to transform from transparent to cloudy was taken as the cloud point. The temperature was then lowered and the sample isothermically annealed until the blend became rehomogenizated. This last method was employed, when possible, to confirm reversibility of the process. The reproducibility of cloud points from several runs was about ±2°C.

4. Results and discussion

4.1. Interaction energies

Blends of PS and PCHMA exhibit miscibility over the entire composition range up to 242°C and show a typical LCST behaviour. Meanwhile, blends of PAMS and PCHMA exhibit miscibility over the entire composition range but do not show LCST behaviour before decomposition temperatures are reached. However, if unsubstituted PS

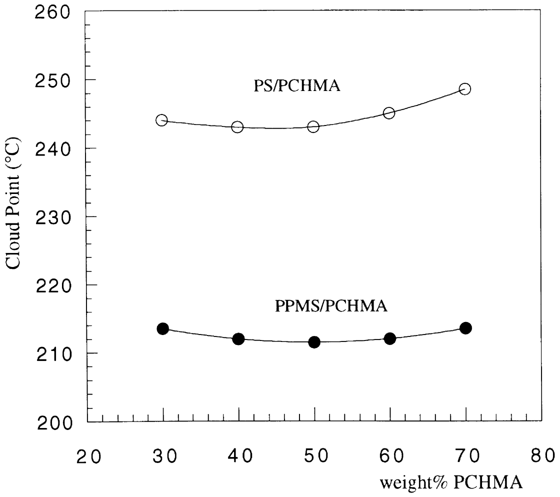

Fig. 2. Cloud point curves for blends of PCHMA with PS (upper) and PPMS (lower).

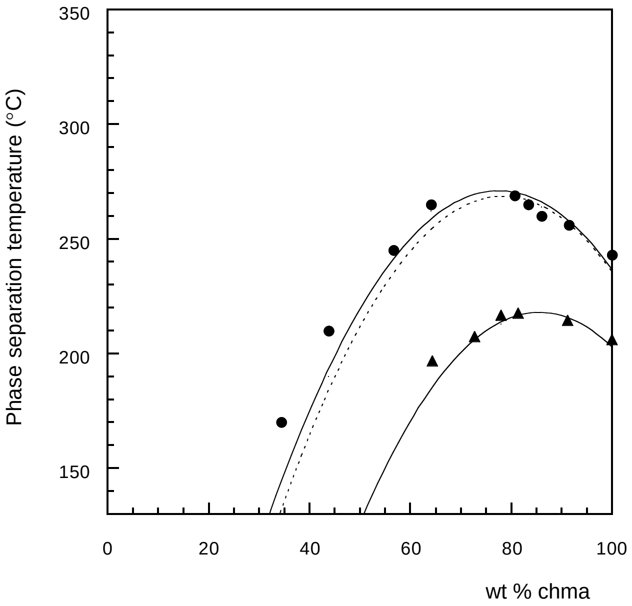

Fig. 3. Phase separation temperatures for 50/50 blends of PS and PPMS with P(CHMA-*co*-MMA) copolymers as a function of CHMA content. The full curve is the estimated spinodal temperature using Eq. (7) with the appropriate parameters from Table 3. Full circles from Nishimoto et al. [2] and triangles from Mugica et al. [23] are the experimentally determined phase separation temperatures. The broken line in the upper curve, represents the estimated spinodal temperature using $\Delta P^*_{\mathrm{S/MMA}} = 0.23$ cal cm^{-3} [24].

is replaced by PPMS, the phase separation temperatures are lowered about 30°C pointing out that subtle differences of the monomer structures have significant influence on LCST behaviour. In Fig. 2 are shown the cloud point curves for PS/PCHMA and PPMS/PCHMA blends, which curves have a broad minimum centred at about 50 wt% PCHMA. The differences among the monomer structures should be captured to a good degree by the interaction energies between monomer pairs. By applying the methodology described in the theoretical section to cloud point data of PS/PCHMA and PPMS/PCHMA blends, the Sanchez–Lacombe equation of state theory, which predicts LCST behaviour, can be used to evaluate the interaction energies between monomer pairs. In this context, the interaction energy of every pair, ΔP^*_{ij} is defined as a 'bare' interaction energy density in which the free volume effects have been stripped away. The obtained values are $\Delta P^*_{\mathrm{S/CHMA}} = -0.16$ and $\Delta P^*_{\mathrm{PMS/CHMA}} = -0.096$ cal cm^{-3}. Considering that the molecular weight of PAMS ($M_w \sim 425\,000$) is higher than PS and PPMS here employed (Table 1), the higher miscibility exhibited by PAMS/PCHMA cannot be due to a more favourable combinatorial entropy of mixing. Thus, as the LCST of PAMS/PCHMA is higher than that of the PS/PCHMA and PPMS/PCHMA blends, it could be expected that $\Delta P^*_{\mathrm{AMS/CHMA}}$ will be more negative than the above values.

This last analysis assumes that experimental phase separation temperatures represent a spinodal curve which, it is well known [22], may not be true; therefore, the values above obtained have to be taken with caution. A set of intersegmental parameters could be considered reliable if that set is capable of reproducing the LCST behaviour of copolymer mixtures with a large number of copolymer compositions. To employ this strategy, accurate LCST data across a wide range of copolymer compositions is required. For this purpose, binary blends of P(CHMA-*co*-MMA) copolymers with PS, PPMS and PAMS have been analysed. The experimental uncertainties in the assigment of cloud points to binodal or spinodal curves are minimized in the critical point where both curves converge. In this study, phase separation temperatures for 50/50 blend compositions were taken as an aproximation to the critical temperature of the mixtures. Fig. 3 shows LCST behaviour for the blends of different copolymer compositions with PS and PPMS. The experimental cloud points showed here for the PS/P(CHMA-*co*-MMA) system were determined by Nishimoto et al. [2] and the cloud points for PPMS/(CHMA-*co*-MMA) were determined by us in a previous paper [23]. For the PAMS/P(CHMA-*co*-MMA) system, most of the cloud points are at temperatures higher than thermal decomposition. This fact prevents the determination of the interaction energy for this system. Fig. 3 shows that there exists a percentage content of MMA in the copolymer, about 20% for PS/P(CHMA-*co*-MMA) and 10% for PPMS/P(CHMA-*co*-MMA), at which LCST is maximized. To obtain the intermolecular interaction parameter, ΔP^*, for homopolymer/copolymer systems, the phase separation temperatures shown in Fig. 3 were fit to Eq. (7) for the spinodal condition derived from Sanchez–Lacombe theory, employing the characteristic parameters given in Table 2. Figs. 4 and 5 show the variation with copolymer composition of ΔP^* so obtained for blends of P(CHMA-*co*-MMA) with PS and PPMS, respectively.

The ΔP^*_{ij} for each binary pair in PS/P(CHMA-*co*-MMA)

Table 2
Sanchez–Lacombe equation-of-state parameters obtained over the range of 0–50 MPa

Repeat unit type	ρ^* (g/cm^3)	P^* (bar)	T^* (K)	Temp range (°C)	Ref.
PS	1.0922	3725	810	220–275	[15,6,25,26]
PMMA	1.246	5001	758	220–270	[15]
PCHMA	1.1624	4429	735	123–198	[27]
PPMS[a]	1.0703	3810	796	139–198	[27]

[a] Values of poly(*o*-methylstyrene) assigned to PPMS based on group contribution theory [28].

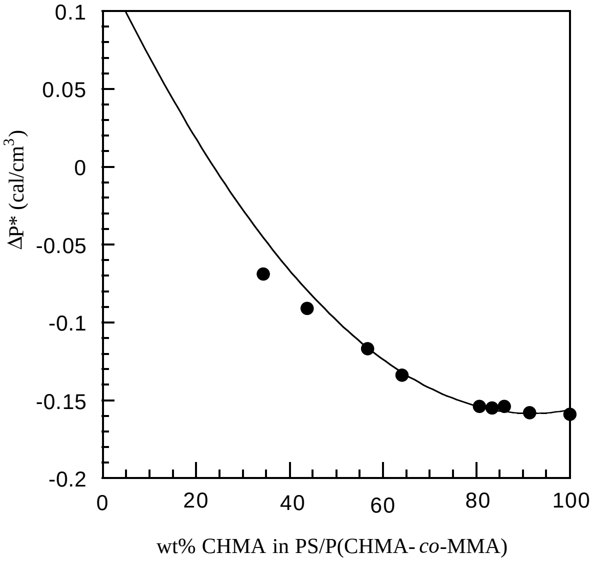

Fig. 4. Effect of copolymer composition on the bare interaction parameter for 50/50 PS/P(CHMA-*co*-MMA) blends. The solid line was calculated by inserting the corresponding parameters from Table 3 into Eq. (6).

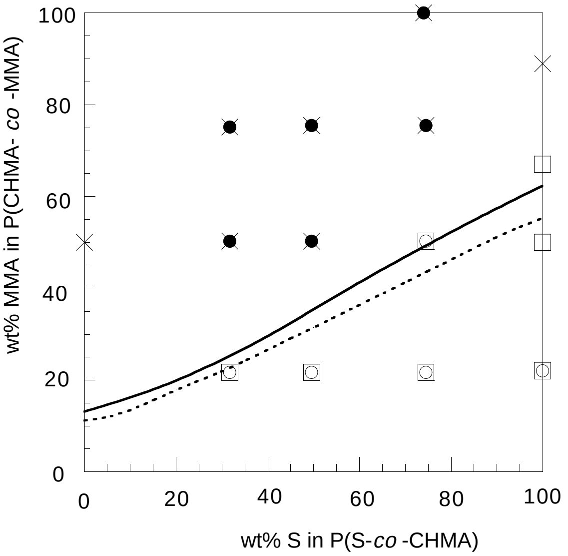

Fig. 6. Miscibility map for 50/50 blends of P(S-*co*-CHMA) copolymers with P(CHMA-*co*-MMA) copolymers at 130°C: (X) opaque, (●) two T_g's, (☐) clear, (○) one T_g. The lines are the miscibility boundaries calculated from Sanchez–Lacombe theory using the parameters from Table 3 for the solid line and $\Delta P^*_{S/MMA} = 0.23$ cal cm^{-3} for the dotted one.

blend system can be determined by linear least-squares fitting of values shown in Fig. 4 to Eq. (6). However, more reliable ΔP^*_{ij} values can be obtained by reducing the degrees of freedom in the fitting process; therefore, we set the value of the $\Delta P^*_{S/MMA}$ parameter, which is one of the most studied in the literature [16,24,29–31]. For this calculation two values were assigned to $\Delta P^*_{S/MMA}$ in the range of those found in the literature, 0.13 and 0.23 cal cm^{-3}. The first one (0.13 cal cm^{-3}) is the same as that obtained by Kim and Paul [16] and similar to $\Delta P^*_{S/MMA} = 0.16$ cal cm^{-3} determined from miscibility maps by Gan and Paul [29] and $\Delta P^*_{S/MMA} = 0.15$ cal cm^{-3} given by Kim and Paul [30]. The highest value employed here, $\Delta P^*_{S/MMA} = 0.23$ cal cm^{-3}, was obtained from other blend systems [24,29,31]. This variety of values could be attributed to different parameters for the equation-of-state employed in the calculations, the diversity in molecular weight of the polymers employed, and also to the inherent difficulties in measuring the experimental cloud points. We examine both values and, in this paper the best reproduction of the experimental LCST points is achieved taking $\Delta P^*_{S/MMA} = 0.13$ cal cm^{-3}, as can be seen in Fig. 3. The remaining

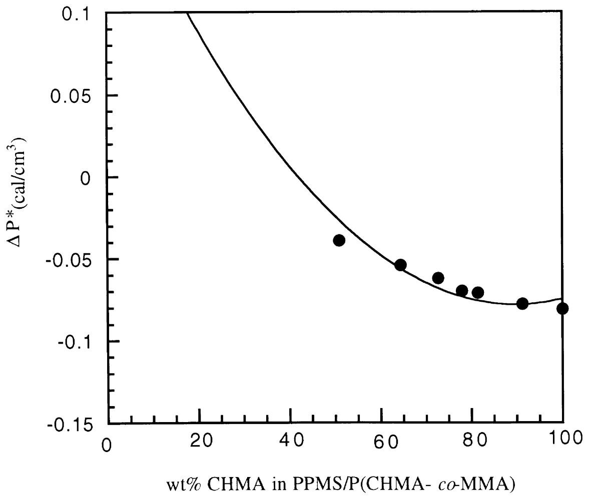

Fig. 5. Effect of copolymer composition on the bare interaction parameter for 50/50 PPMS/P(CHMA-*co*-MMA) blends. The solid line was calculated by inserting the corresponding parameters from Table 3 into Eq. (6).

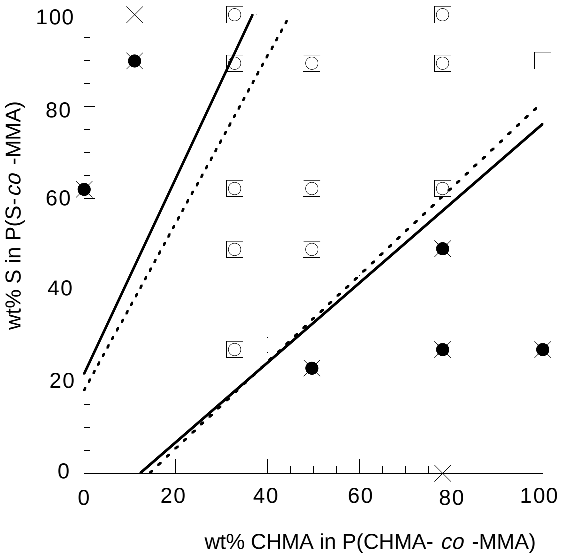

Fig. 7. Miscibility map for 50/50 blends of P(S-*co*-MMA) copolymers with P(CHMA-*co*-MMA) copolymers at 130°C: (X) opaque, (●) two T_g's, (☐) clear, (○) one T_g. The lines are the miscibility boundaries calculated from Sanchez–Lacombe theory using the parameters from Table 3 for the solid line and $\Delta P^*_{S/MMA} = 0.23$ cal cm^{-3} for the dotted one.

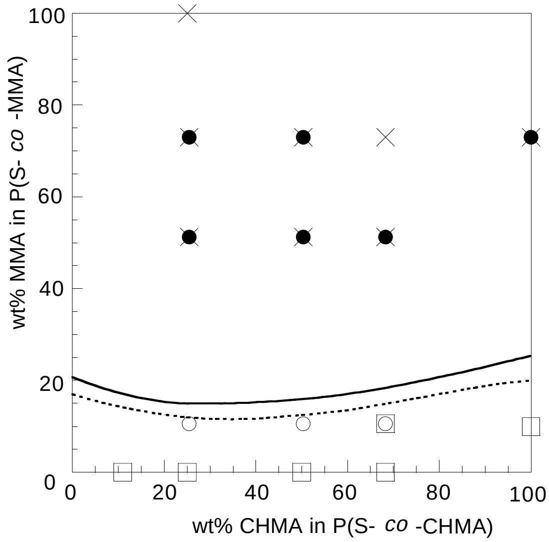

Fig. 8. Miscibility map for 50/50 blends of P(S-*co*-MMA) copolymers with P(S-*co*-CHMA) copolymers at 130°C: (X) opaque, (●) two T_g's, (☐) clear, (○) one T_g. The lines are the miscibility boundaries calculated from Sanchez–Lacombe theory using the parameters from Table 3 for the solid line and $\Delta P^*_{S/MMA} = 0.23$ cal cm^{-3} for the dotted one.

binary interaction energies are given in Table 3. The interaction parameter for the S/CHMA pair (-0.157 cal cm^{-3}) is in good agreement with that obtained above from cloud points of PS/PCHMA blend (-0.16 cal cm^{-3}). $\Delta P^*_{MMA/CHMA}$ was found to have a positive value as expected because PCHMA and PMMA are immiscible. The repulsive intramolecular interaction between CHMA and MMA units promotes the blend miscibility of PS/P(CHMA-*co*-MMA). The binary interaction parameters obtained from LCST of the PPMS/P(CHMA-*co*-MMA) system were similarly calculated by a linear least square fitting of the ΔP^*_{ij} in Fig. 5 to Eq. (6). As before, more reliable values of ΔP^*_{ij} can be obtained if in the fitting process some of interaction energies are known. In this case, we set $\Delta P^*_{CHMA/MMA} =$ 0.34 cal cm^{-3} which was determined from the blend system PS/P(CHMA-*co*-MMA) analysed above. The results are given in Table 3.

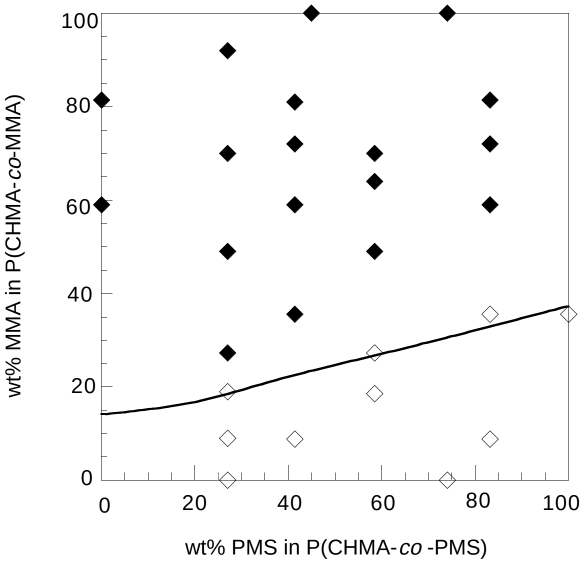

Fig. 9. Miscibility map for 50/50 blends of P(CHMA-*co*-PMS) copolymers with P(CHMA-*co*-MMA) copolymers at 130°C: (◆) opaque, (◇) clear. The solid line is the spinodal calculated from Sanchez–Lacombe theory using the parameters from Table 3.

Analysing the 'bare' interaction parameters obtained in this paper, we can observe that small changes in repeat unit structure, e.g. PPMS relative to polystyrene, apparently decrease the strength of their interactions with PCHMA and PMMA. In summary, the use of PPMS in place of polystyrene decreases the width of the miscibility window and lowers the phase separation temperatures for blends with PCHMA or P(CHMA-*co*-MMA). This can be appreciated in both Figs. 2 and 3.

Turning our attention to PAMS, blends of PCHMA with PAMS show no phase separation curve before their decomposition. This important feature and the knowledge of the parameter $\Delta P^*_{AMS/MMA} = 0.02$ cal cm^{-3} [24] indicate that PAMS will probably interact more favourably with PCHMA and PMMA than PS and PPMS do. In conclusion, while the inclusion of a methyl group in the para position in the styrene repeat unit apparently decreases the strength of the interactions with PCHMA and PMMA, the inclusion of a methyl group in the alpha position has the opposite effect. These results agree with those obtained by the authors in a previous work [23].

For polymer blend systems, there exist few miscibility maps which compare theoretical predictions using the equation-of-state theory, with experimental results [31–33]. In this paper, the interaction parameters obtained by the equation-of-state theory, Table 3, have been employed to predict isothermal miscibility maps of binary blends involving copolymers of S, PMS, CHMA, and MMA (Figs. 6–11). Theoretical miscibility maps and experimental data show good agreement for all systems. Moreover, one can see that miscibility maps for copolymers involving PMS show smaller miscibility area than the maps involving S. This behaviour, as it is seen in Figs. 2 and 3, and in previous papers [23,34], supports the statement that the position of the methyl group in the styrene repeat unit plays an important role in macroscopic blend miscibility. It is noticeable too, that miscibility windows of systems involving copolymers of S are better fit to using the experimental data $\Delta P^*_{S/MMA} = 0.13$ instead of $\Delta P^*_{S/MMA} = 0.23$ cal cm^{-3}.

4.2. Equation-of-state effects

Assuming that ΔP^* and the equation-of-state parameters of the polymers employed are not a function of temperature, B_{sc} can be calculated at any temperature for the interacting pairs using ΔP^*_{ij} from Table 3 and Eq. (13) as shown by Kim and Paul [15]. As expected, the value of $B_{S/MMA}$ so calculated (0.16 cal cm^{-3}) is the same as that reported by Gan and Paul [29] and similar to the value reported by Fukuda et al.

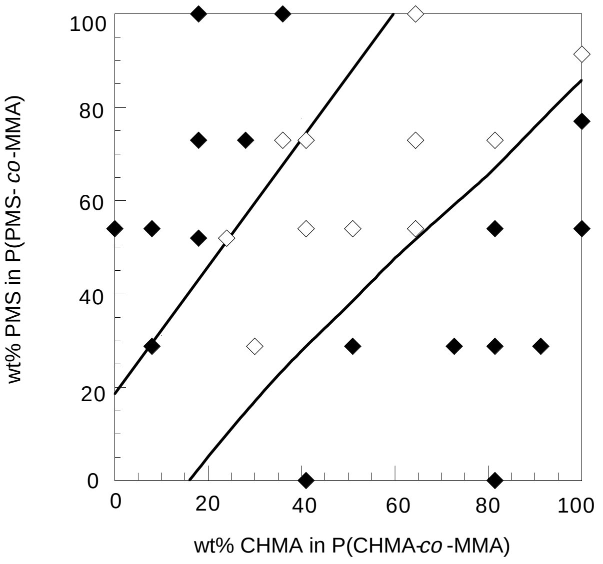

Fig. 10. Miscibility map for 50/50 blends of P(PMS-*co*-MMA) copolymers with P(CHMA-*co*-MMA) copolymers at 130°C: (◆) opaque, (◇) clear. The solid line is the spinodal calculated from Sanchez–Lacombe theory using the parameters from Table 3.

[35–37] (0.18 cal cm^{-3}). Moreover, the $B_{\mathrm{S/CHMA}}$ value of -0.05 cal cm^{-3} determined in this paper is in good agreement with the value of -0.03 cal cm^{-3} reported by Chu and Paul [31]. However, $B_{\mathrm{CHMA/MMA}} = 0.32$ cal cm^{-3} calculated here does not match well with either of the two values reported by Chu and Paul [31] (0.73 and 0.80–0.87 cal cm^{-3}). Overall, the agreement with those authors can be considered quite good taking into account the characteristic parameters used in those papers are different from those employed by us.

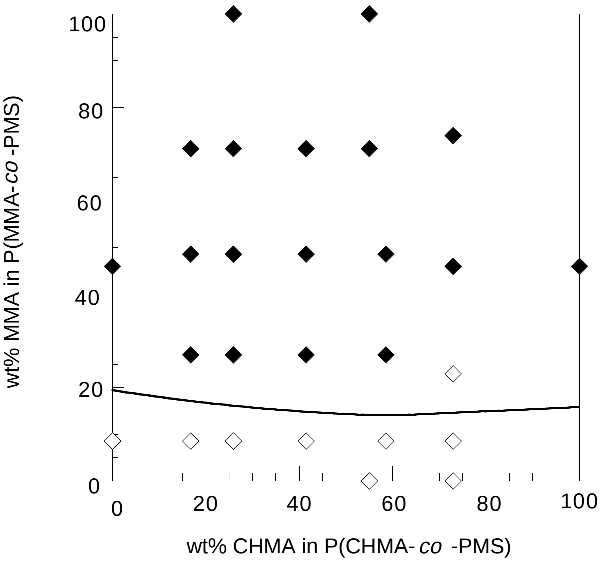

Fig. 11. Miscibility map for 50/50 blends of P(CHMA-*co*-PMS) copolymers with P(MMA-*co*-PMS) copolymers at 130°C: (◆) opaque, (◇) clear. The solid line is the spinodal calculated from Sanchez–Lacombe theory using the parameters from Table 3.

The differences between $B_{\mathrm{sc}}(130°\mathrm{C})$ and ΔP_{ij}^* obtained in this work (Table 3) reflect the effect of equation-of-state contributions. For high molecular weight polymers the equation corresponding to the spinodal condition (Eq. (7)) can be reduced to

$$\frac{\mathrm{d}^2G}{\mathrm{d}\phi_1^2} = -\frac{\tilde{\rho}\Delta P^* v^*}{kT} - \frac{\tilde{\rho}}{2}\left[\frac{\nu(T_1^* - T_2^*)}{T(\phi_1 + \nu\phi_2)^2}\right]^2 \tilde{T}P^*\beta = 0 \tag{14}$$

The explanation for the observed phase behaviour in PS/PCHMA and PPMS/PCHMA blend systems is revealed by the two terms in the spinodal equation (Eq. (14)) that comprise the stability condition. The first term could be positive or negative depending on the sign of ΔP_{ij}^* but it is a weak function of temperature. However, the second term is in relation with the equation-of-state effects and destabilizes the mixture at any temperature. Both the interaction energy (ΔP^*) and the equation-of-state effect (ΔT^*) can cause phase separation. For blends of PS or PPMS with PCHMA, according to the values obtained for the above terms ($\Delta P^*_{\mathrm{S/CHMA}} = -0.16$, $\Delta P^*_{\mathrm{PMS/CHMA}} = -0.08$ cal cm^{-3}, $\Delta T^*_{\mathrm{S/CHMA}} = 75$ and $\Delta T^*_{\mathrm{PMS/CHMA}} = 61$ K), the phase separation would be mainly driven by the large difference in the T_i^* values. This means that the equation-of-state effects for these systems are the main cause of the LCST behaviour. On the other hand, the dominant factor which affects the difference in the phase separation temperatures exhibited by those systems is the difference in the ΔP_{ij}^* values ($\Delta P^*_{\mathrm{S/CHMA}} = -0.16$ and $\Delta P^*_{\mathrm{PMS/CHMA}} = -0.08$ cal cm^{-3}) obtained for each blend system. Note that although these values seem very similar at first sight, a small difference between them has a large effect on the phase separation temperature. Furthermore, for the homopolymer/copolymer blend systems here studied (PS/P(CHMA-*co*-MMA) and PPMS/P(CHMA-*co*-MMA)), there is a competition among the above two terms (ΔP^* and ΔT^*) (Eq. (14)) when copolymer composition is varied. Increasing MMA content in the P(CHMA-*co*-MMA) copolymer causes a decrease in the ΔT^* of the system which is favourable for phase stability, whereas the ΔP^* value increases which is clearly unfavourable for miscibility. In consequence, at low content of MMA there is a small composition range (MMA wt% 0–20) where phase separation temperature increases as MMA content goes up. At higher contents of MMA blend stability decreases strongly leading to immiscibility in PS/P(CHMA-*co*-MMA), as well as in PPMS/P(CHMA-*co*-MMA) blend systems. In summary, although the equation of state effects are the dominant factor in determining the LCST behaviour of the systems above described for the majority of the copolymer composition range, the differences in the phase separation temperatures between blends of PS and PPMS depend upon the different values in the bare interaction parameters obtained for each one, which are influenced by the inclusion of a methyl group in the styrene repeat unit.

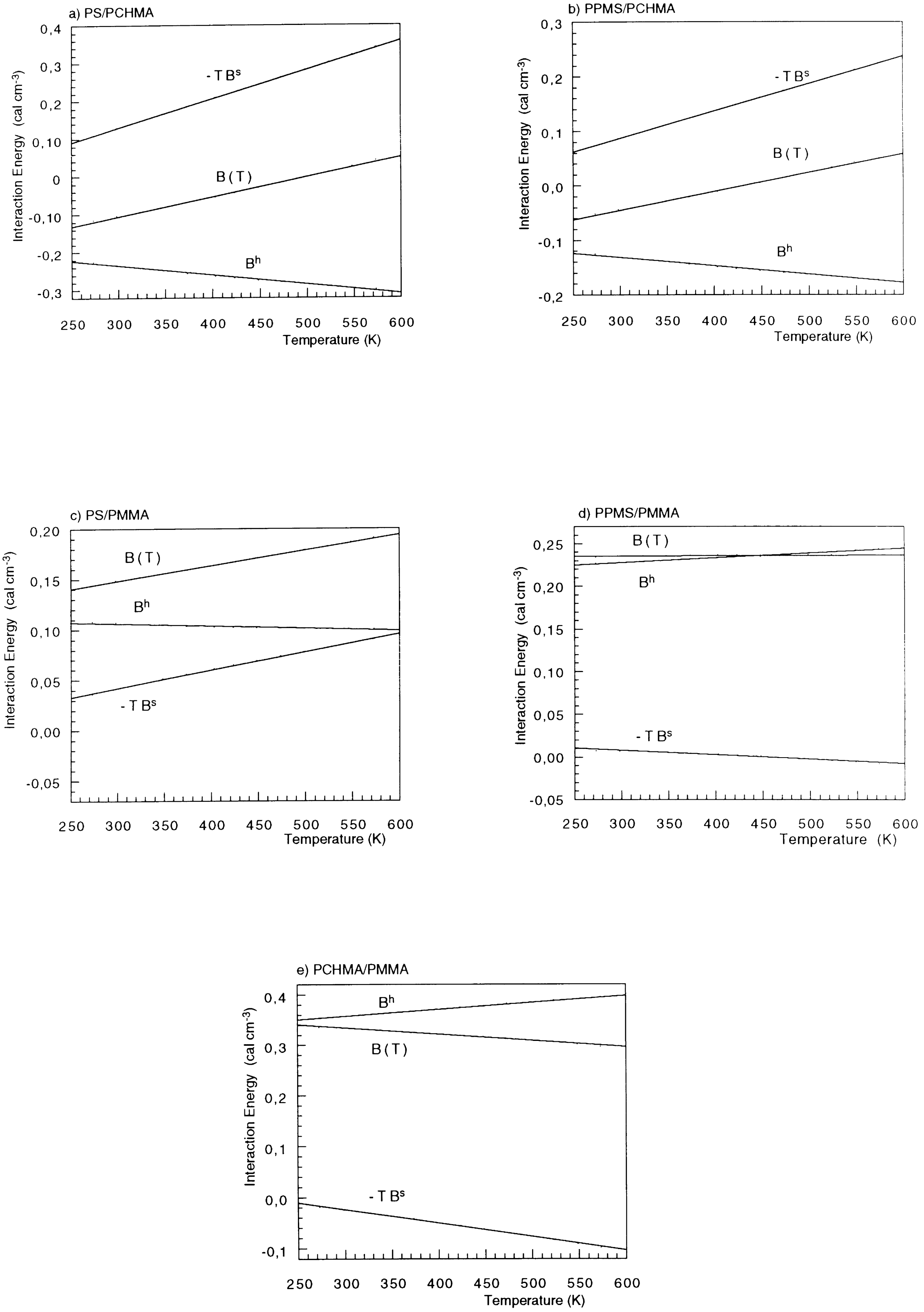

Fig. 12. Effect of temperature on the extended Flory–Huggins interaction energy and its enthalpic and entropic components for 50/50 blends: (a) PS/PCHMA; (b) PPMS/PCHMA; (c) PS/PMMA; (d) PPMS/PMMA; and (e) PCHMA/PMMA.

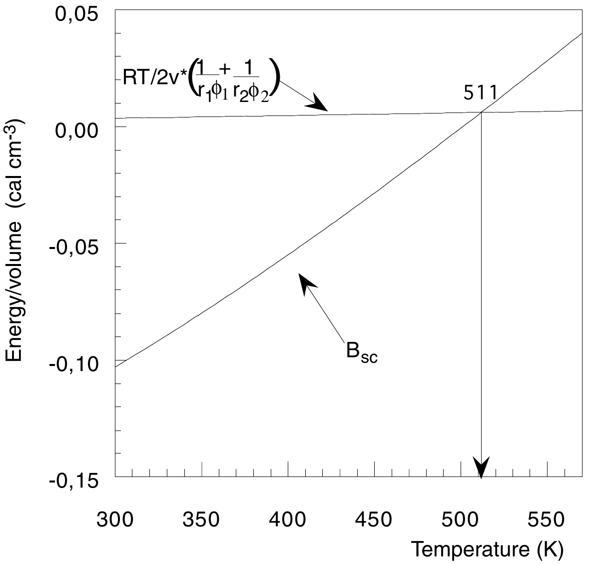

Fig. 13. Temperature dependence of B_{sc} and the combinatorial entropy term at the spinodal condition for 50/50 PS/PCHMA blend. The intersection of the two lines corresponds to the spinodal temperature. The brackets contain the experimental value obtained by visual assessment.

The Sanchez–Lacombe theory can be used to compute the temperature dependent Flory–Huggins interaction parameter, $B(T)$, its enthalpic part, B^h, and the entropic one, $-TB^s$, from Eqs. (10)–(13). A key assumption is that the bare interaction energy, ΔP^*, has been assumed to be independent of temperature which is believed to be quite reasonable for blends where only weak interactions exist [13,15,16,24,29,38–41]. Therefore, the temperature dependence of $B(T)$ should be due to equation-of-state effects. Fig. 12 shows how B^h, B^s and $B(T)$ vary with temperature for: (a) PS/PCHMA; (b) PPMS/PCHMA; (c) PS/PMMA; (d) PPMS/PMMA; and (e) PCHMA/PMMA 50 wt% composition blends. The term B^h, which is related to the heat of mixing, becomes slightly more negative for PS/PMMA, PS/PCHMA and PPMS/PCHMA systems as temperature increases whereas the entropic term, $-TB^s$, becomes larger and more positive. This last behaviour is in concordance with the thermodynamic analysis made by Sanchez [42], who argues that thermally induced phase separation is entropically driven.

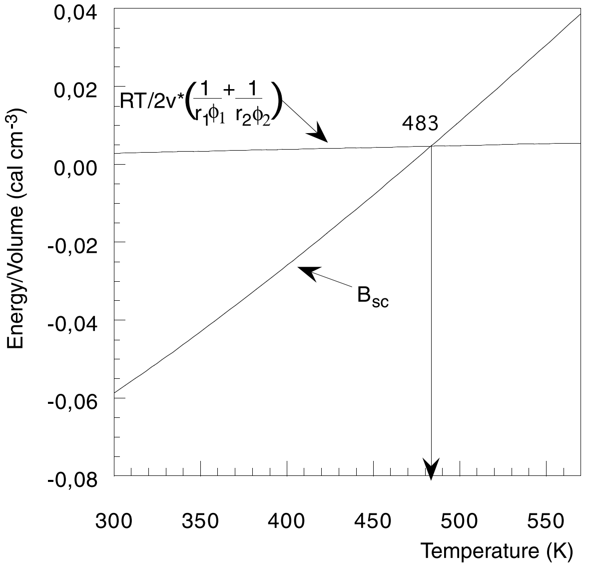

Fig. 14. Temperature dependence of B_{sc} and the combinatorial entropy term at the spinodal condition for 50/50 PPMS/PCHMA blend. The intersection of the two lines corresponds to the spinodal temperature. The brackets contain the experimental value obtained by visual assessment.

If we compare the evolution with temperature of the two terms, combinatorial entropy and B_{sc} (calculated from the Sanchez–Lacombe theory), of Flory–Huggins theory (Eq. (12)) the intersection of these two lines gives us the spinodal point where phase separation occurs as required by the spinodal condition. Figs. 13 and 14 show this intersection point for PS/PCHMA and PPMS/PCHMA 50 wt% blends, respectively. This can be compared to experimental LCST points in Fig. 2. It is remarkable that if the bare interaction parameter $\Delta P^*_{\mathrm{PMS/CHMA}} = -0.096\ \mathrm{cal\ cm^{-3}}$, obtained from the PPMS/PCHMA blend system (Fig. 2), is used instead of the value $\Delta P^*_{\mathrm{PMS/CHMA}} = -0.08\ \mathrm{cal\ cm^{-3}}$ obtained from the PPMS/P(CHMA-*co*-MMA) blend system (Fig. 3), we get a LCST temperature which agrees better with experimentally determined phase separation temperature (see Fig. 2). This behaviour could be explained taking into account that as the interaction parameters obtained for these systems are very small, predicted phase separation temperature would be extremely sensitive to the ΔP^*_{ij} used. Upon considering the errors in the experimental measurements, as well as the various assumptions made in the Sanchez–Lacombe lattice fluid model (i.e. mean field approximation [41] and the neglect of the surface area effect [43]) the agreement found here between experiment and theory is notable.

5. Summary

Repeat unit interaction energies of both PS and PPMS with CHMA and MMA, and also of these last two with each other were evaluated from the LCST type phase behaviour using the lattice fluid theory of Sanchez and Lacombe. This work includes estimates for the binary interaction of PMS with MMA and CHMA reported here for the first time. The other three interaction energy values ($\Delta P^*_{\mathrm{S/CHMA}}$, $\Delta P^*_{\mathrm{S/MMA}}$ and $\Delta P^*_{\mathrm{CHMA/MMA}}$) calculated here are consistent with values reported previously in other sources. The values of ΔP^* were used to map composition boundaries between miscibility and immiscibility in copolymer systems, Figs. 6–11. This mapping agrees very well with the experimental points obtained. All results indicate that small change in repeat unit structure, e.g. *p*-methylstyrene relative to styrene, decreases the strength of the interaction with CHMA and narrows the miscibility region. The 'bare' interaction parameters obtained in this paper, given in Table 3, agree with these conclusions.

Table 3
Interaction parameters (cal cm^{-3}) determined in this study

Interaction pair	ΔP_{ij}^*	B_{SC} at 130°C
S–MMA	0.13	0.16
S–CHMA	−0.16	−0.05
PMS–MMA	0.23	0.24
PMS–CHMA	−0.08	−0.01
CHMA–MMA	0.34	0.32

Based on thermodynamic analysis of blends of PS or PPMS with PCHMA and P(CHMA-*co*-MMA), we found that phase separation was mainly driven by the equation-of-state effects due to great difference in the T_i^* values. Moreover, the optimum comomer content of MMA in P(CHMA-*co*-MMA) for the most favourable interaction with PS or PPMS (around 25% for PS and 15% for PPMS) is dominated by the equation-of-state effects while the weak intramolecular repulsion between CHMA and MMA units is a minor factor.

The differences in the phase separation temperatures between blends of PS or PPMS due to the inclusion of a methyl group in the styrene repeat unit, can not be explained by the equation-of-state effects; the differences in the phase separation temperatures is attributed to the different values in the bare interaction parameters determined for each one. Furthermore, the analysis of the evolution with temperature of thermodynamic functions representing the blend (i.e. the interaction energy density (B_{sc}), and its enthalpic (B^h) and entropic components ($-TB^s$)) shows us the capability of lattice fluid theory to predict and explain the LCST behaviour of the systems studied in this paper without any empirical correction.

Finally, an in-depth conformational study of the polymers used in this paper would be desirable to complete the understanding of the influence on blend packing had by the addition of a methyl group in the styrene repeat unit.

Acknowledgements

We are pleased to acknowledge financial support of this work by Gobierno Vasco (PI 96/59), as well as the University of the Basque Country (project no. UPV 203.215- G41-98). The authors wish to thank A. Etxeberria PhD, for the development of the computer programs used.

References

[1] Brannock GR, Barlow JW, Paul DR. J Polym Sci Polym Phys 1990;28:871.
[2] Nishimoto M, Keskkula H, Paul DR. Macromolecules 1990;29:3633.
[3] Hseih DJ, Peiffer DG, Rabeony M, Siakali-Kioulafa E, Hadjichristidis N. Macromolecules 1993;26:4979.
[4] Gan PP, Paul DR, Padwa AR. Polymer 1994;35:1501.
[5] Kim CK, Paul DR. J Polym Sci Polym Phys 1996;34:2641.
[6] Flory PJ. Principles of polymer chemistry, Ithaca, NY: Cornell University Press, 1953.
[7] Brannock GR, Paul DR. Macromolecules 1990;23:5240.
[8] Schweizer KS, Curro JG. J Chem Phys 1989;91:5059.
[9] Flory PJ, Orwoll RA, Vrij A. J Am Chem Soc 1964;86:3507.
[10] Flory PJ. Discuss Faraday Soc 1970;49:7.
[11] Patterson D, Robard A. Macromolecules 1978;11:690.
[12] Lacombe RH, Sanchez IC. J Phys Chem 1976;80:2568.
[13] Sanchez IC, Lacombe RH. Macromolecules 1978;11:1145.
[14] Kim JH, Barlow JW, Paul DR. J Polym Sci Polym Phys Ed 1989;27:223.
[15] Kim CK, Paul DR. Polymer 1992;33(8):1630.
[16] Kim CK, Paul DR. Polymer 1992;33(10):2089.
[17] Kambour RP, Bendler JT, Bopp RC. Macromolecules 1983;16:753.
[18] ten Brinke G, Karasz FE, MacKnight WJ. Macromolecules 1983;16:1827.
[19] Paul DR, Barlow JW. Polymer 1984;25:487.
[20] Coleman MM, Graft JF, Painter PC. Specific interactions and the miscibility of polymer blends, Lancaster, PA: Technomic, 1991.
[21] Bershtein VA, Egorov V. Differential scanning calorimetry of polymers, New York: Ellis Horwood, 1994.
[22] Olabisi O, Robeson LM, Shaw MT. Polymer–polymer miscibility, New York: Academic Press, 1979.
[23] Mugica A, Barral M, Pomposo JA, Cortazar M. Acta polym 1999;50:304.
[24] Gan PP, Paul DR, Padwa AR. Polymer 1994;35(7):1487.
[25] Merfeld GD, Paul DR. Polymer 1998;39(10):1999.
[26] Gan PP, Paul DR. J Appl Polym Sci 1994;54:317.
[27] Rodgers PA. J Appl Polym Sci 1993;48:1061.
[28] Boudouris D, Constantinou L, Panayiotou C. Ind Eng Chem Res 1997;36:3968.
[29] Gan PP, Paul DR. Polymer 1994;35(16):3513.
[30] Kim CK, Paul DR. Polymer 1992;33(23):4941.
[31] Chu JH, Paul DR. Polymer 1999;40:2687.
[32] Merfeld GD, Paul DR. Polymer 1998;39(10):1999.
[33] Merfeld GD, Chan K, Paul DR. Macromolecules 1999;32:429.
[34] Pomposo JA, Mugica A, Areizaga J, Cortazar M. Acta Polym 1998;49:301.
[35] Fukuda T, Nagata M, Inagaki H. Macromolecules 1984;17:548.
[36] Fukuda T, Inagaki H. Pure Appl Chem 1983;55:1541.
[37] Fukuda T, Nagata M, Inagaki H. Macromolecules 1986;19:1411.
[38] Callaghan TA, Paul DR. Macromolecules 1993;26:2439.
[39] Callaghan TA, Paul DR. J Polym Sci Polym Phys 1994;32:1813.
[40] Sanchez IC, Lacombe RH. J Polym Sci 1977;15:71.
[41] Sanchez IC, Lacombe RH. J Phys Chem 1976;80:2352.
[42] Sanchez IC. Encyclopedia of physical science and technology, XI. New York: Academic Press, 1987. p. 1.
[43] Rudolf B. Polymer 1996;37(5):825.